JNC TN8400 2003-024

Experimental and Modeling Studies on Gas Migration in Kunigel V1 Bentonite

(Research Document)

Nobember, 2003

Japan Nuclear Cycle Development Institute
Tokai Works

〒319-1184　茨城県那珂郡東海村村松４番地４９
核燃料サイクル開発機構
技術展開部　技術協力課
電話：029-282-1122（代表）
ファックス：029-282-7980
電子メール：jserv@jnc.go.jp

JNC TN8400 2003-024
November, 2003

Experimental and Modeling Studies on Gas Migration in Kunigel V1 Bentonite

(Research Document)

Kenji TANAI*, Mikihiko YAMAMOTO**

Abstract

The knowledge obtained from previous studies are as follows, i) The gas permeabilities are 10^{-17} m^2 for the 30wt% sand mixtures at a dry density of 1.6 Mg m^{-3} and 10^{-20} to 10^{-21} m^2 for the bentonite (100%) at a dry density of 1.8 Mg m^{-3}, ii) The breakthrough pressure seems to be almost the same as the swelling pressure at constant volume condition, iii) Gas pathways created during the first gas injection period are closed due to bentonite swelling during the resaturation period.

For the recent experiment, two peaks of gas flow rate are obtained. In particular, maximum flow rate at the secondary peak is obtained approximately 1,667 cc min^{-1}. This peak is probably indicative of generation of cracks in the specimen by particle displacement. Breakthrough pressure (2.5 MPa) is lager than the swelling pressure of the bentonite (swelling pressure is approximately 1.0 MP at a dry density of 1.6 Mg m^{-3}). It may be that there is a time lag between the gas pressure change in the clay and expansion of cracks due to large pumping rate (0.05 cc min^{-1}). The gas migration pathways are unstable due to stress condition in bentonite specimen and/or heterogeneity of specimen.

The distribution of bulk density in the specimen was measured to demonstrate that X-ray CT was reliable new technique for the non-destructive measurement of gas migration through bentonite specimen. The degree of X-ray attenuation depends on the bulk density of the bentonite specimen. The change in bulk density in this test specimen is not clarified from this test case. These experimental results are probably indicative of migration along preferential pathway rather than uniform flow in the matrix of bentonite specimen.

A modified TOUGH2 simulator which has a gas flow model based on Kozeny-Carman relationship was developed and applied to simulate of gas migration test in compacted bentonite. Although the results of the simulation reasonably agreed with obtained experimental data around gas breakthrough phenomenon, it has some difficulties to simulate "burst flow" which has extremely large and instantaneous increase of gas out flow. From these results, despite these difficulties, the continuous approach which can be conveniently coupled with phenomena of mechanical nature is one of the potential methods of describing gas migration in clay material.

---

* Barrier performance group, Waste isolation research division,
Waste management and fuel cycle research center, Tokai works
** Toyo Engineering Corporation

JNC TN8400 2003-024
2003 年 11 月

クニゲル V1 ベントナイト中のガス移行に関する試験及び解析的検討（研究報告）

棚井　憲治*　山本　幹彦**

要　旨

これまでに行ったガス移行試験の結果から，以下のような知見が得られた。

1) ガスの有効浸透率は，ベントナイト 70%＋ケイ砂 30%混合試料で乾燥密度 1.6Mg m^{-3} の場合 10^{-17} m^2，ベントナイト単一材料で乾燥密度 1.8mg m^{-3} の場合 10^{-20} から $10^{-21}m^2$ 程度である。
2) 体積拘束型の試験におけるガス破過圧力は，ほぼ膨潤応力と等しい。
3) ガスの移行によって形成された経路は，ベントナイトの有する膨潤性能により閉塞する。

また，最新のガス移行実験結果から 2 つのピークが得られた。特に，2 回目のピーク時におけるガスの透過流量としては，最大 1667cc min^{-1} という値であった。このようなピークが得られた理由としては，ベントナイト粒子のずれによって試料中に亀裂が生成されたものと推測される。なお，本試験で得られた破過圧力は，膨潤応力よりも大きな値となっており，ガス移行経路生成の時間遅れ，ならびに供給時のガス流量に起因した亀裂の拡張などが影響しているものと考えられる。いずれにしろ，ガス移行経路の形成は，試料の応力状態や試料そのものの不均一性などに影響され変化しやすいことがいえる。

ガス移行試験中における試料内の密度変化の測定を目的に X 線 CT による非破壊試験を行った。本試験は X 線の吸収係数が，媒体の密度に比例して変化することを利用したものである。試験の結果，試料中の密度変化は明確に現れなかったが，これらの結果から試料中をガスが均一に流れているというよりは，選択的な経路を移行していることを示していると考えられる。

ガス移行可視化試験の結果を対象として TOUGH2 改良コードによる解析を実施し，Kozney-Carman モデルを応用した改良型モデルによりガス破過時の挙動をほぼ表現できうる結果となった。しかしながら，2 回目のピークに見られるようなダイナミックな流動に関しては，それを表現することが非常に困難であることが分った。

---

*　東海事業所　環境保全・研究開発センター　処分研究部　処分バリア性能研究グループ
**　東洋エンジニアリング株式会社

Table of contents

List of Tables

List of Figures

1. Introduction

Carbon steel is a candidate for the overpack materials of geological disposal of high-level waste in Japan. The corrosion of the carbon steel overpack in aqueous solution under anoxic conditions will be accompanied by the generation of hydrogen gas, which may affect hydrological and mechanical conditions of the bentonite buffer. To evaluate the consequences of gas generation on radioactive waste repository in deep underground, it is necessary to develop a gas migration model for bentonite buffer material based on the information obtained from experiments.
The objective of this study is to obtain an understanding of the gas migration mechanism through bentonite.
This paper presents a description of the knowledge of previous study and current status of gas migration study in JNC.

2. Previous studies (Tanai et al., 1997 : JNC, 2000)

2.1 Experimental outline

In order to evaluate gas migration behaviour in buffer material, experiments are conducted on swelling buffer samples under saturated condition. This is necessary because it is assumed that the buffer material is saturated by groundwater at the time of gas generation by overpack corrosion. Bentonite (100%) and bentonite/sand mixtures material (70wt% bentonite +30wt% sand) are used as experimental materials. The set up of the test apparatus is shown schematically in Figure-1. Buffer samples are placed in the test vessel and compacted uniaxially to predetermined dry densities. Water is supplied from the lower side of specimen by water-head method or water injection pump. Hydrogen gas is injected from the lower side of the specimen and injection pressure is increased stepwise up to a pressure at which breakthrough occurs. In these experiments, the breakthrough pressure and gas flow rate are measured continuously. All tests are conducted at room temperature conditions.

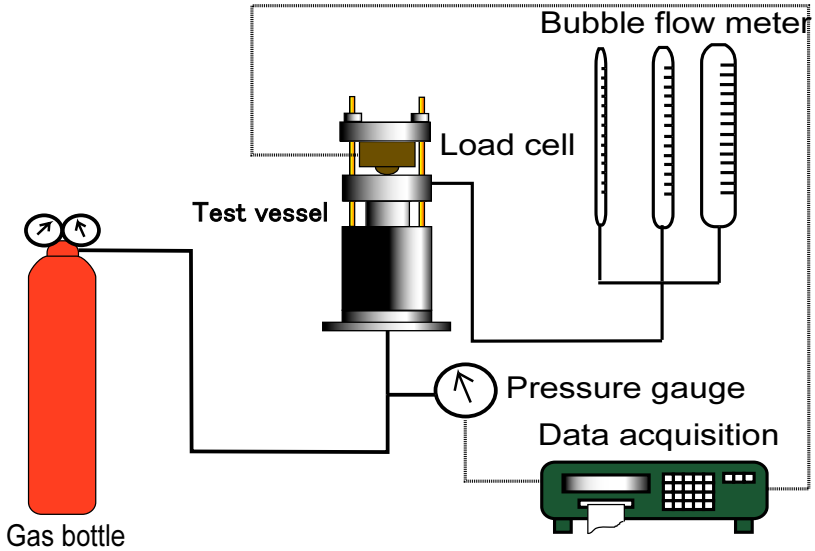

Figure-1 Outline of experimental apparatus

2.2 Results of previous study

2.2.1 Gas permeability

The measured results of gas permeability as function of effective clay density are shown in Figure-2. The gas permeability, K_g, is calculated by the following equation;

$$Kg = \frac{2Q\mu PL}{A\left(P_i^2 - P_o^2\right)} \quad (1)$$

where K_g is the gas permeability [m^2], Q is the gas flow rate [$m^3\ s^{-1}$], μ is the viscosity of gas [Pa s], P is the pressure at which the flow rate is measured [Pa], L is the specimen thickness [m], A is cross sectional area of specimen [m^2], P_i is the absolute injection pressure [Pa], and P_o is the absolute exit pressure [Pa].

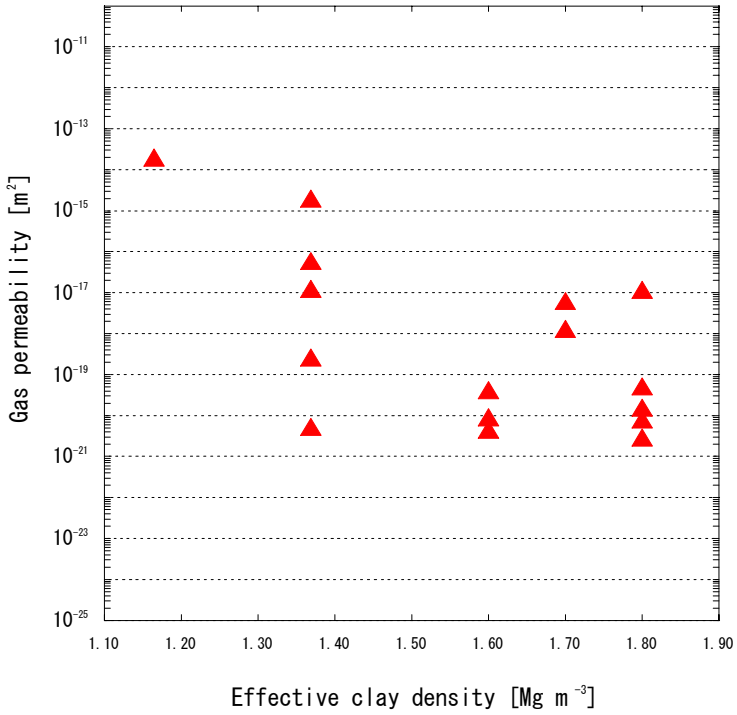

Figure-2 Relationship between effective clay density and gas permeability

Figure-2 shows that as expected, the gas permeability for pure bentonite and bentonite/sand mixture materials tends to decrease as effective clay density increases.
In any case, gas flow rate gradually shifts to dynamic flow from leisurely flow (a very small amount flow) through specimen. And, data dispersion is probably indicative of influence of heterogeneity of the specimen and/or experimental conditions such as method of increasing gas pressure etc,. The gas permeabilities obtained are 10^{-17} m^2 for the 30wt% sand mixtures at a dry density of 1.6 Mg m^{-3} and 10^{-20} to 10^{-21} m^2 for the bentonite (100%) at a dry density of 1.8 Mg m^{-3}.

2.2.2 Relationship between breakthrough pressure and swelling pressure

The relationship between breakthrough pressure and swelling pressure obtained is shown in Figure-3. The relationship between the swelling pressure (σ [MPa]) and effective clay density (ρ_e [Mg m^{-3}]) obtained from swelling test of bentonite can be expressed by the

following (JNC, 2000);

$$\text{Distilled water condition:}\quad \sigma = \exp(3.8497\rho_e^2 - 7.333\rho_e + 2.0856) \tag{2}$$

$$\text{Synthetic seawater:}\quad \sigma = 3.7952\times10^{-5}\exp(6.4482\rho_e) \tag{3}$$

The breakthrough pressure seems to be almost the same as the swelling pressure from experimental results. On the other hand, the breakthrough pressure with 10 cm thick sample is more than twice as large as the pressure with the 1 and 5 cm thick samples. It may be that there is a time lag between the gas pressure change in the clay and the expansion of cracks that serve as the gas pathways as the sample thickness increases. In other words, the formation of the gas migration pathways occurs too late to follow the pressure rise, which resulted in the high breakthrough pressure. The gas pressure is increased in steps of 7 to 10 days in this test. The gas may breakthrough at the swelling pressure of the buffer material if the rate of increase in pressure of the gas between the overpack and buffer increases slowly.

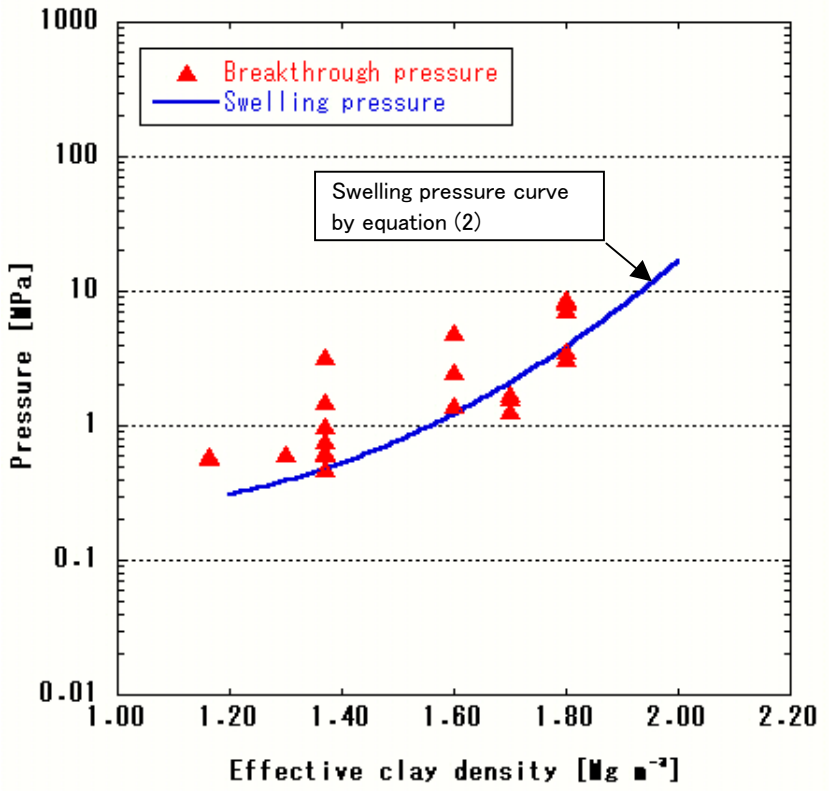

Figure-3 Relationship between swelling pressure and breakthrough pressure

2.2.3 Recovery of gas pathways

It is assumed that gas first accumulates at the overpack-buffer interface, followed by gas migration through the buffer occurring repeatedly during the operational life time of an actual repository. It is important to evaluate if the gas migration pathway, once formed, can recover by the self-sealing ability of bentonite. The reproducibility of the gas breakthrough pressure is measured to estimate the recovery of gas pathways. Results of tests are shown in Table-1. As to reproducibility of the breakthrough pressure, it is observed that first and second breakthrough pressure are almost the same for the specimens. This suggests that gas pathways created during the first gas injection period are closed due to bentonite swelling during the resaturation period.

Table-1 Repeatability of the breakthrough pressure

Test No.	Breakthrough pressure	
	First step	Second step
1	8.88 MPa	8.14 MPa
2	0.60 MPa	0.59 MPa
3	0.62 MPa	0.65 MPa
4	3.59 MPa	3.15 MPa
5	1.64 MPa	1.70 MPa

3. Current status of gas migration study

Any basic knowledge for gas migration behaviour in bentonite was obtained from previous studies. However, new gas migration test using X-ray CT technique performed to more clarify the gas migration behaviour in bentonite. And, an analysis by the modified TOUGH2 code using gas migration test result performed to evaluate of applicability of this model.
For the first item, distribution of bulk density of bentonite specimen was measured to demonstrate that X-ray CT was a reliable new technique for the non-destructive measurement of the gas migration behaviour in bentonite.

3.1 Gas migration test

3.1.1 Test apparatus
(1) Gas migration test apparatus
The set up of the gas migration test apparatus is shown schematically in Figure-4. This apparatus comprises four main components: (a) a specimen assembly, (b) fluid injection system together with its associated pressure control pump, (c) a backpressure system, and (d) a microcomputer-based data acquisition system. The clay is equilibrated by backpressuring with distilled water at a fixed pressure. A 3.8 cm diameter cylindrical clay specimen is placed between sintered stainless steel porous filters.

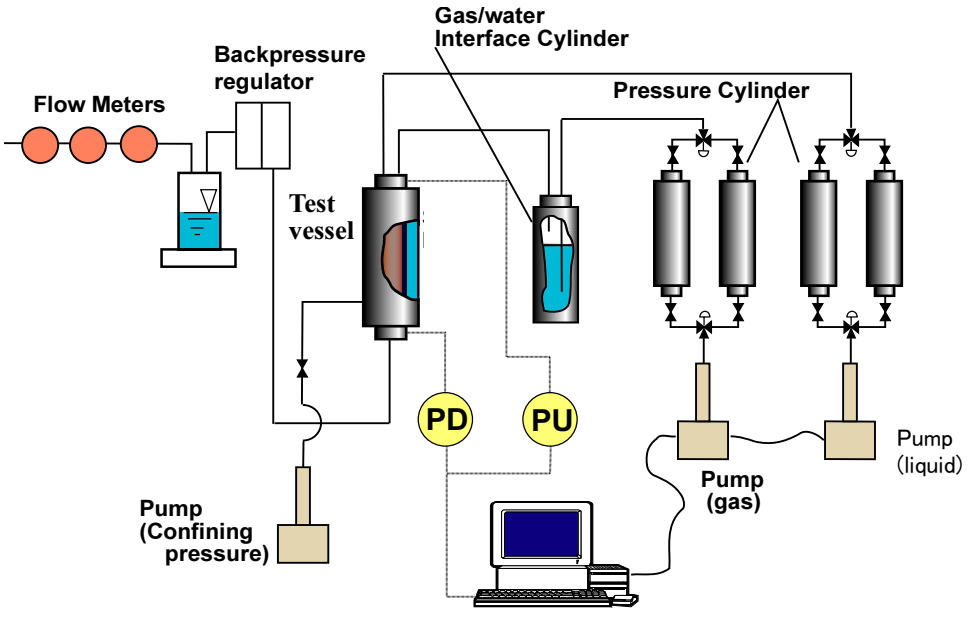

Figure-4 Schematic of the gas migration test apparatus

(2) X-ray CT scanner

An X-ray CT scanner, Asteion VI (Toshiba Medical Co.) was used in this test. It is the third –generation medical scanner (Figure-5). A target in an X-ray tube is attacked by electrons accelerated at 135 kV with a 200 mA current. An X-ray fan-beam from the tube penetrates a sample on a bed made of carbon. The intensity of the X-ray beam after the sample penetration is measured by 896 detectors. The expose time of X-ray is 1.0 sec (time for the 360° rotation of the X-ray tube). The time for the image reconstruction by Fourier transformation is 3.0 sec. The degree of X-ray attenuation increases linearly with the bulk density of sample. Figure-6 shows relationship between bulk density and CT value of Kunigel V1 bentonite. It is realized from this figure that the CT value is well correlated with density of the materials. The bulk density of Kunigel V1 bentonite, ρ_b is obtained by the following equations:

$$\rho_b = (CT + 1465.7)/1495.6 \quad \text{[CT : CT value for the specimen]} \tag{4}$$

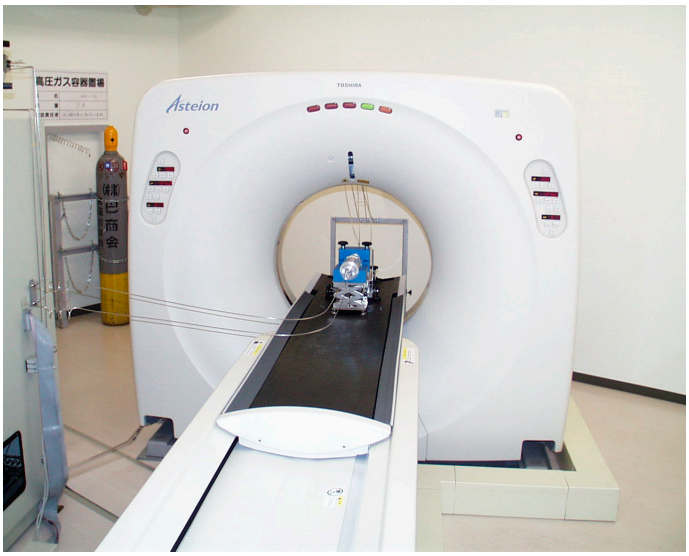

Figure-5 X-ray CT scanner (Asteion VI)

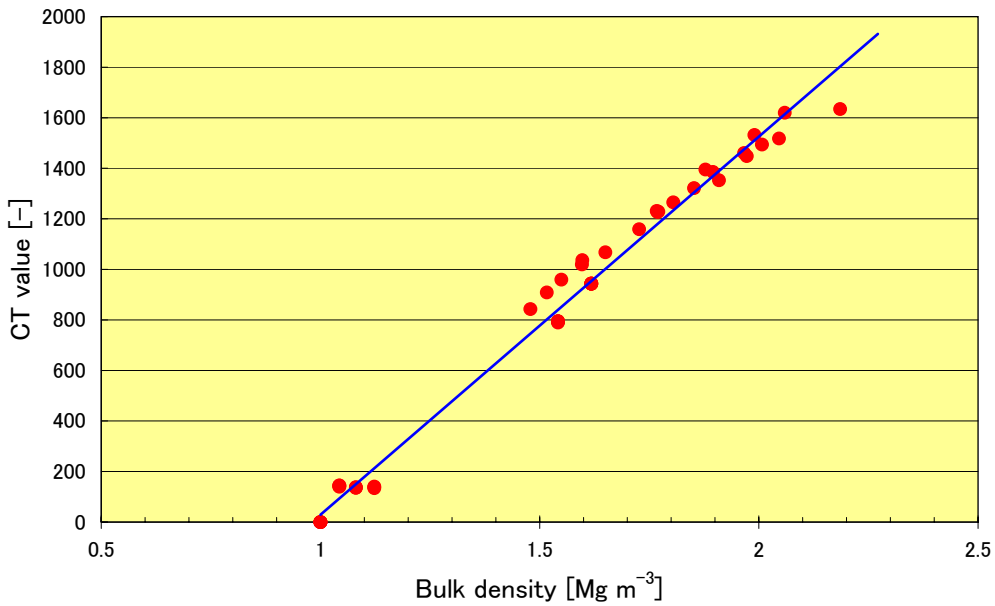

Figure-6 Relationship between bulk density and CT value of Kunigel V1 bentonite

3.1.2 Test procedures

Bentonite powder is placed in the test vessel and compacted uniaxially to dry density of 1.6 Mg m^{-3}. Water was supplied from the upstream of the specimen by water injection pump. After saturated of the specimen, helium was admitted into the upper part of the gas-water interface cylinder and the tubing and porous disc were gas-flushed. The initial gas pressure in the injection system was set using a regulator (initial pressure of approximately 600 kPa). The injection pump was set to constant flow rate mode and pumping rate of 0.05cc min^{-1} (= 3000μL hr^{-1}) was used in this test. In this experiment, the breakthrough pressure, gas flow rate and drainage volume of water are measured continuously. All tests are conducted at room temperature conditions (approximately 20 °C). Test conditions are given in Table-2.

For the X-ray CT measurement, distribution of liquid or gas saturation was measured to demonstrate that X-ray CT was a reliable new technique for the non-destructive measurement of the gas migration behaviour in bentonite. The procedure of the X-ray CT measurement is as follows;

1) measurement of the initial condition (water saturated condition) of the bentonite specimen
2) measurement of the gas injection condition any period of time

The scanning condition shows Table-3.

Table-2 Experimental conditions

material	Kunigel V1 bentonite
specimen size	ϕ 3.8 cm x H 2.0 cm
dry density	1.6 Mg m^{-3}
porosity	0.415
gas injection method	Constant flow rate (0.05cc min^{-1})
backpressure	Atmospheric pressure
confining pressure	Atmospheric pressure
temperature	Room temperature (20 °C)
type of liquid	Distilled water

Table-3 Scanning condition by X-ray CT

power of X-ray tube	135 kV, 200 mA
scan speed	0.75 sec (360° rotation)
thickness of slice	1.0 mm
scan mode	Helical scan

3.1.3 Experimental results

(1) Gas migration test

Figure-7 shows all history of gas pressure and gas flow rate in this test. Figure-8 and Figure-9 shows gas pressure and gas flow rate history after a period of 22days and from 22.8 days to 23 days, respectively. A very small amount of flow was observed at a gas pressure of 2.5 MPa (Figure-8). Gas pressure continued to rise until major gas entry occurred at a gas pressure of 2.6 MPa (Figure-8), accompanied by a increase of gas flow rate. Differential gas pressure and gas flow rate after breakthrough was spontaneously decreased to 22.87 days (Figure-9). Breakthrough pressure is lager than the swelling pressure of the bentonite

(swelling pressure is approximately 1.0 MP at a dry density of 1.6 Mg m^{-3}). And, the secondary peak of gas flow rate occurs at pressure of approximately 1.8 MPa (22.88 days). Maximum gas flow rate at this point was approximately 1667 cc min^{-1}. After the secondary peak, steady-state gas flow was observed at a pressure of approximately 0.67 MPa. This pressure is below a swelling pressure of this specimen. The gas permeabilities obtained are 3.8 to 6.0 x 10^{-20} m^2 at pressure of 2.5 MPa and 9.9 x 10^{-16} m^2 at pressure of approximately 1.8 MPa (Figure-10). The secondary peak is probably indicative of generation of cracks in the specimen by particle displacement.

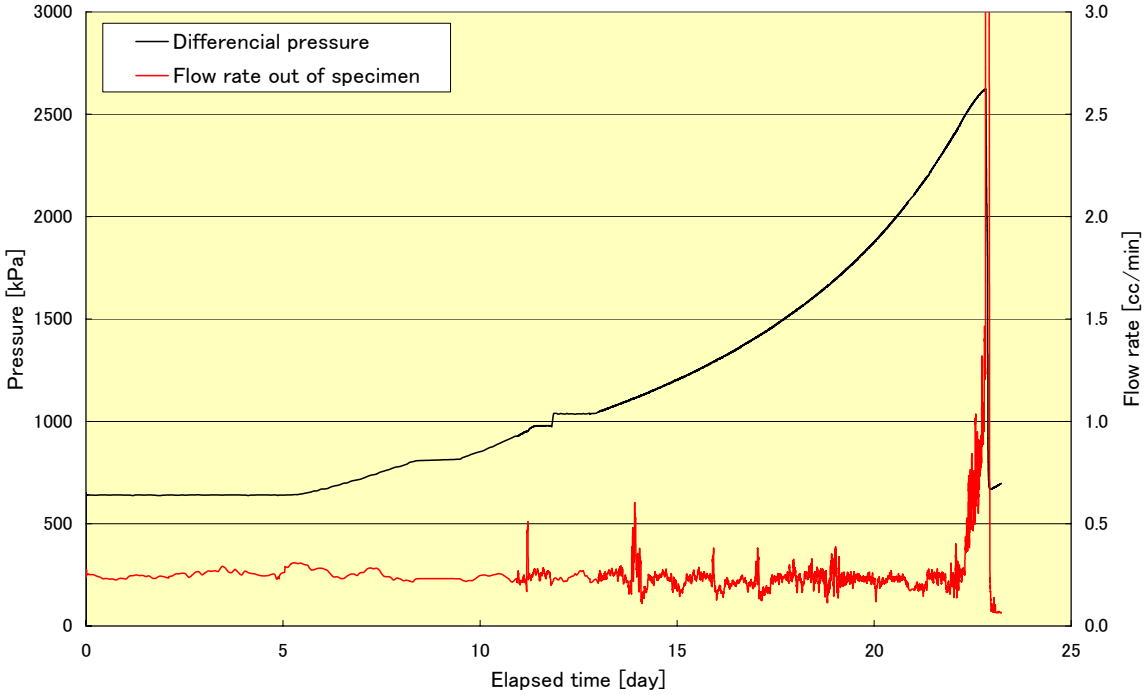

Figure-7 Gas pressure and gas flow rate history

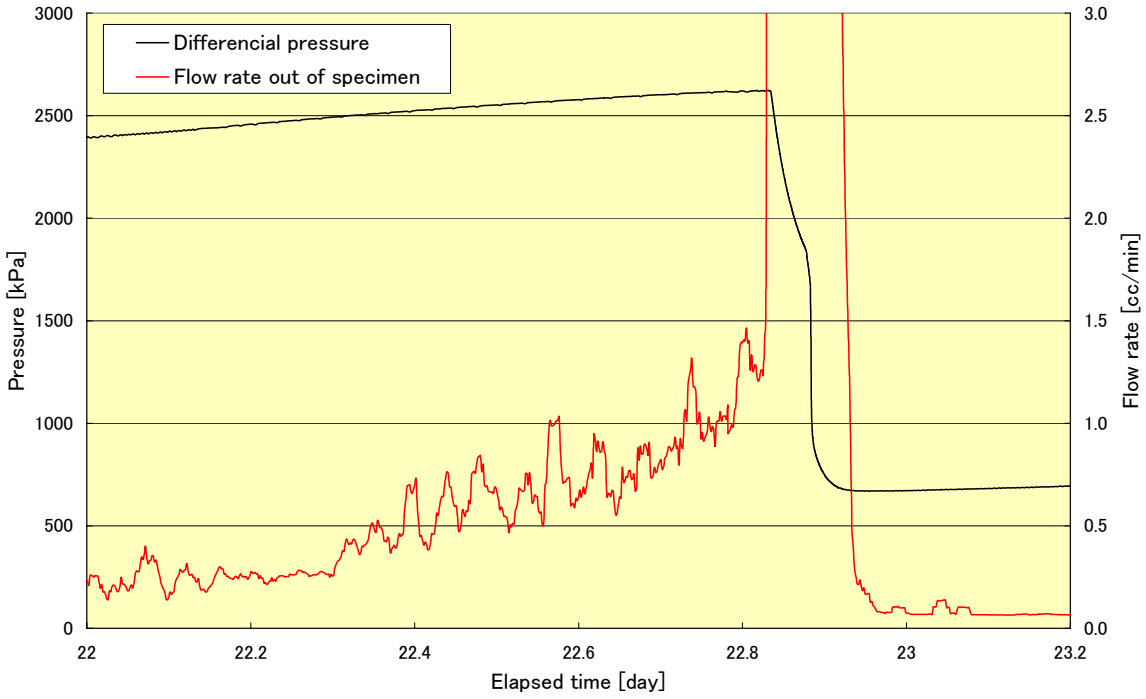

Figure-8 Gas pressure and gas flow rate history after a period of 22 days

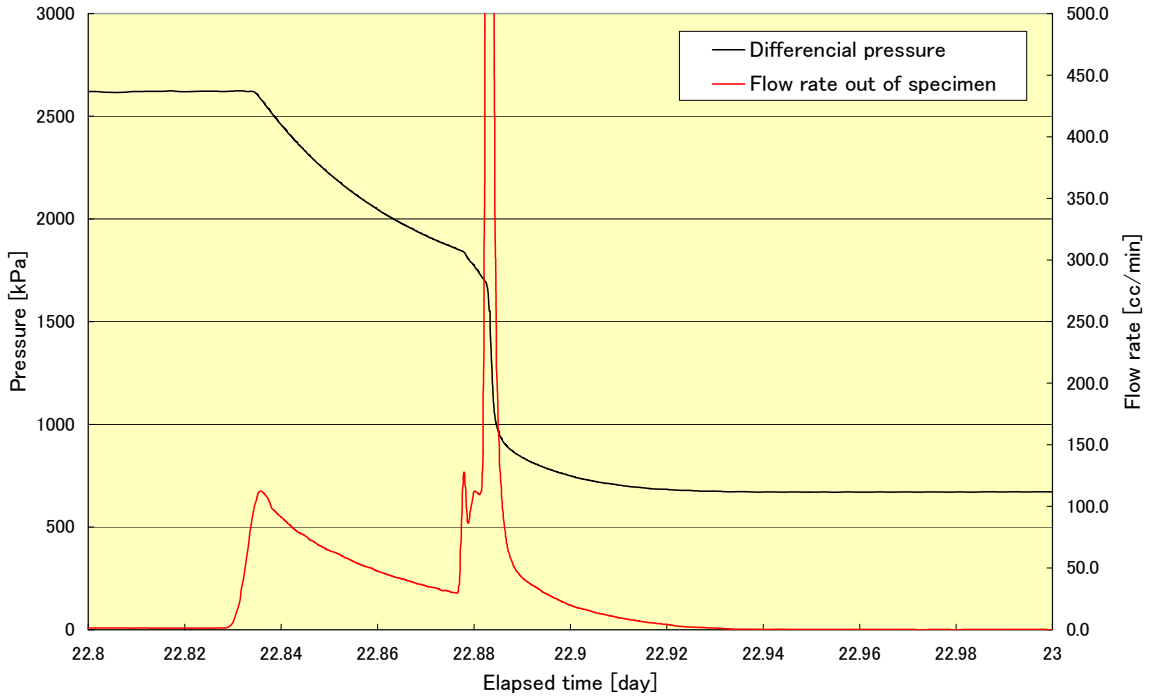

Figure-9 Gas pressure and gas flow rate history from 22.8 days to 23 days

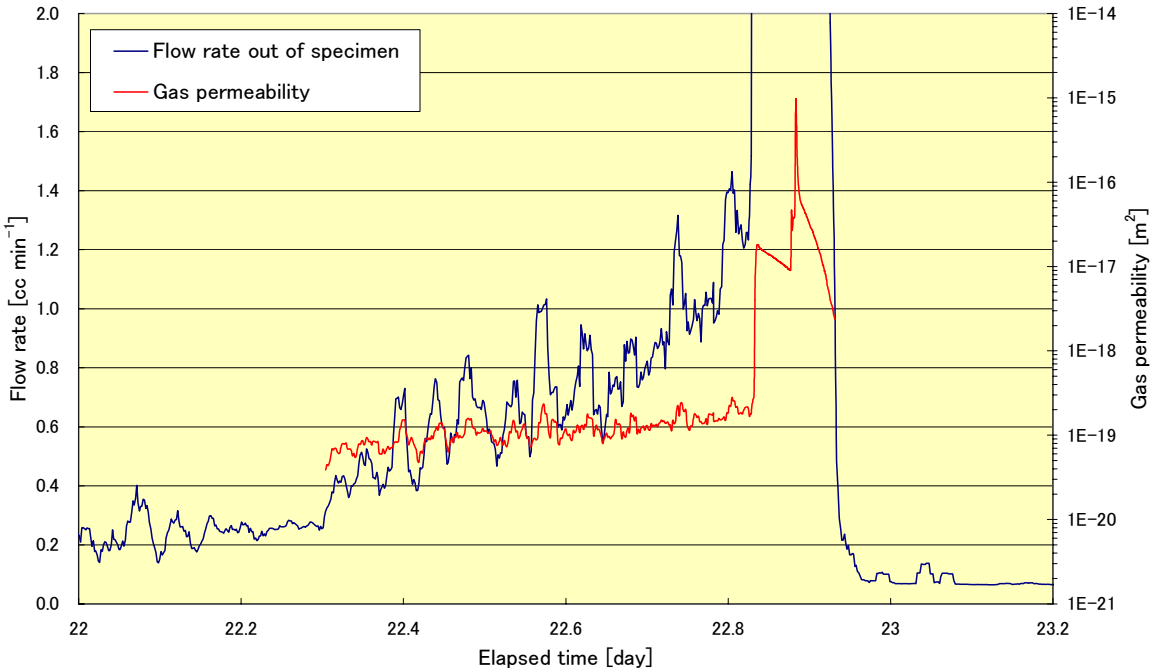

Figure-10 Gas flow rate and gas permeability history after a period of 22 days

(2) CT measurement

The distribution of liquid saturation was measured to demonstrate that X-ray CT was reliable new technique for the non-destructive measurement of gas migration through bentonite specimen. The 2D images of the CT value distribution are shown by Figure-11, 12 and 13. Figure-11 shows the initial condition of the specimen before gas injection. Figure 12 and 13 shows breakthrough point and secondary peak point, respectively. Contrast differences in

the CT images represent bulk density differences in the bentonite specimen. The degree of X-ray attenuation depends on the bulk density of the bentonite specimen (Figure-6). Figure-13 shows line profile of CT value at center position of Figure-10, 11 and 12 images.
The alteration of bulk density in this test specimen is not clear from these results.
The digital data of this CT value obtained from X-ray CT scanner usually includes any kinds of noise. Therefore, this should be excluded in order to obtain clear images and line profile after CT value processing analysis.
Anyhow, these experimental results are probably indicative of migration along preferential pathway rather than uniform flow in the matrix of bentonite specimen.

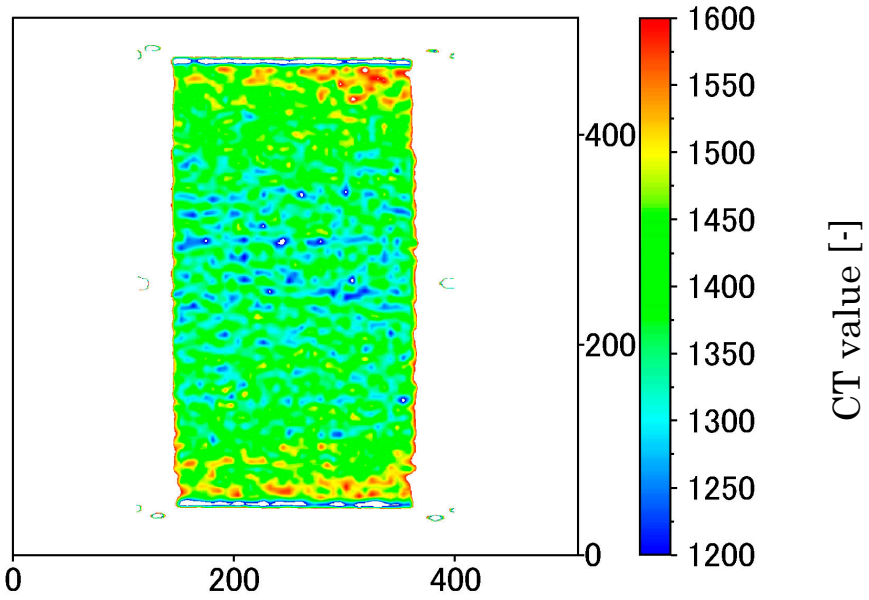

Figure-11 Image of the CT value distribution at initial condition (before gas injection)

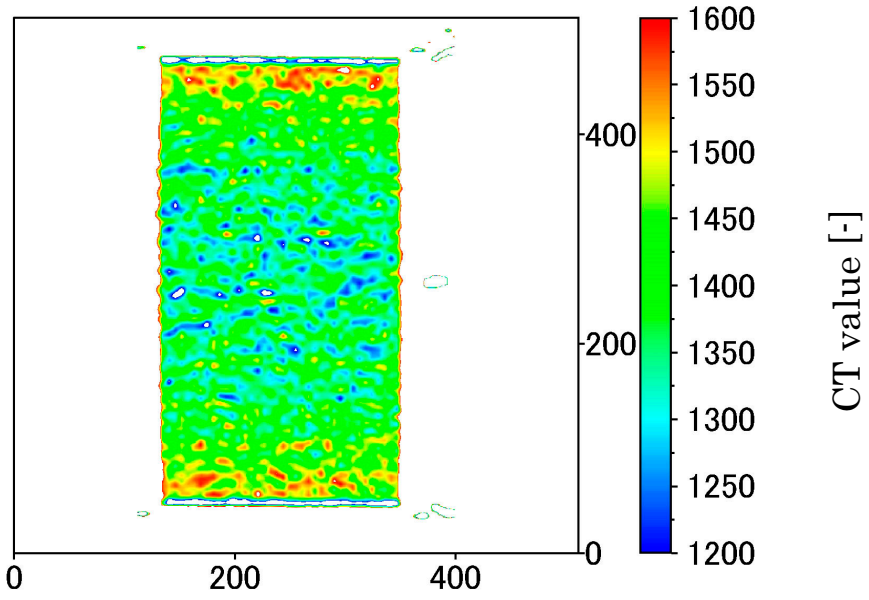

Figure-12 Image of the CT value distribution at breakthrough point

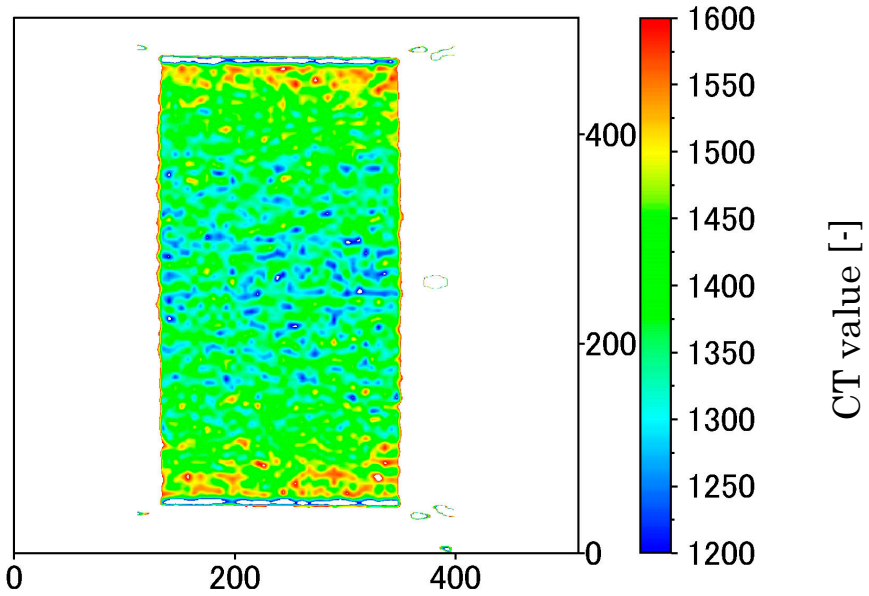

Figure-13 Image of the CT value distribution at secondary peak point
(dynamic flow condition)

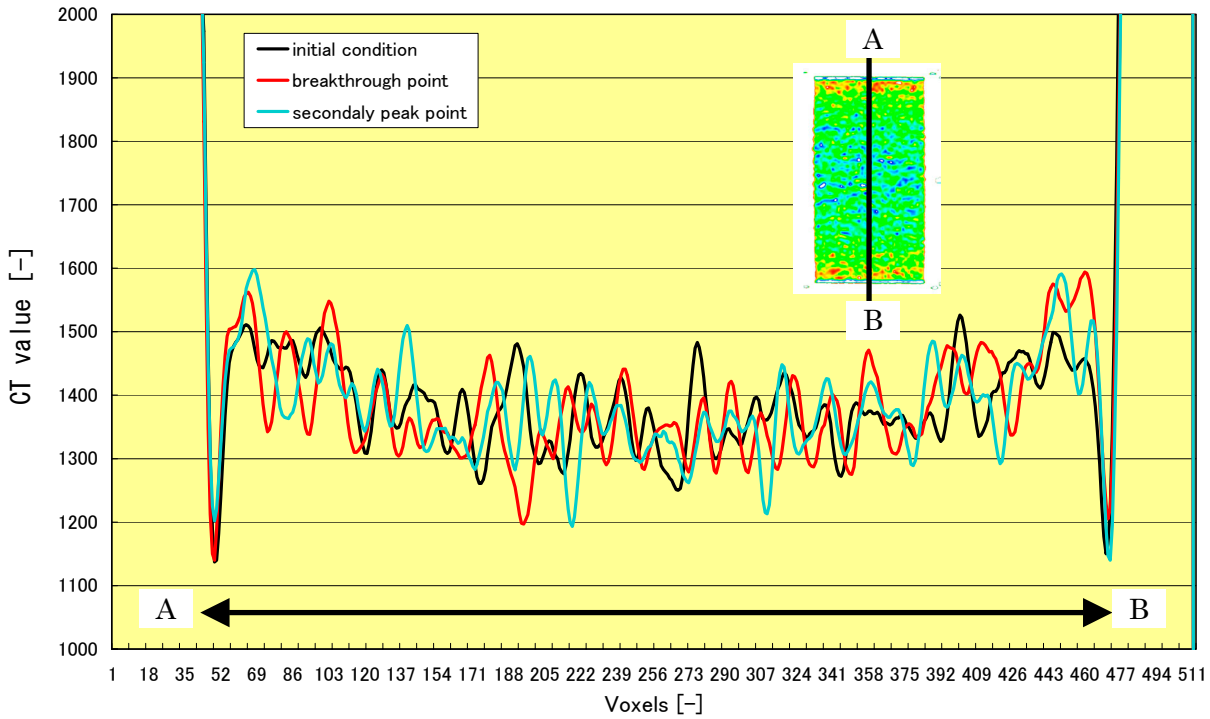

Figure-14 Line profile of CT value of the bentonite sample

3.1.4 Simulation of the gas migration test by modified TOUGH2

Numerical simulation of two-phase porous-medium flow has been applied to simulation of gas out-flow rate obtained from the gas migration test of compacted bentonite.

(1) Outline of modified TOUGH2 code

Conventional porous medium two-phase flow model is not suitable to model gas flow through the compacted bentonite in its original form, because it is unable to represent particular characteristics of gas migration in compacted bentonite. These characteristics observed in experiments so far are

- The opening and closing of gas pathways characterized by two critical pressures: a 'gas-entry pressure', which has to be exceeded before gas flow is started, and a 'shut-in pressure', below which the pathways seal, returning the gas permeability of the bentonite to zero. Both critical pressures are influenced by the clay's state of stress.
- The dependence of the gas permeability on applied gas pressure, which is thought to arise from the opening and closing or dilation and constriction of pathways with changing pressure, is represented by a functional dependence of the gas permeability on gas pressure.
- The time-lag or hysteresis behaviour observed in the relationship between gas permeability and applied gas pressure, that is caused by change of the rate at which the gas permeability changes in response to a change in gas pressure.

In this modification, these characteristics were represented in a two-phase porous-medium model by rather simple method, that is de-coupling the water and gas flows, and by introducing a relative permeability of gas that matches the obtained experimental results. The following enhancements were implemented in TOUGH2. A new module extends the standard TOUGH2 program to model flow through bentonite, and includes molecular diffusion for all components in the gaseous and aqueous phases.

The equation of mass balance for each component in the bentonite domain is

$$\frac{d}{dt}\int_{V_n}\phi\sum_{\beta=1}^{N}\left(\rho_\beta S_\beta X_\beta^{(\kappa)}\right)\mathrm{d}V = \int_{\Gamma_n}\sum_{\beta=1}^{N}\left(\rho_\beta \mathbf{u}_\beta X_\beta^{(\kappa)} - \rho_\beta D_\beta^{(\kappa)}\nabla X_\beta^{(\kappa)}\right)\cdot\mathbf{n}\,\mathrm{d}\Gamma + \int_{V_n} q^{(\kappa)} dV \qquad (5)$$

and

$$\mathbf{u}_\beta = -\frac{\mathbf{k}}{\mu_\beta}k_{r\beta}\left(\nabla P_\beta - \rho_\beta \mathbf{g}\right) \qquad (6)$$

where

β	indicates the phase (i.e. gas, aqueous)
ρ_β	is the density of phase β (kg m^{-3})
ϕ	is the porosity
S_β	is the saturation of phase β
$X_\beta^{(\kappa)}$	is the mass fraction of component κ present in phase β
$D_\beta^{(\kappa)}$	is the effective diffusion coefficient of component κ present in phase β(m^2 s^{-1})
$\mathbf{u}_\beta$	is the Darcy velocity of phase β (m s^{-1})
$\mathbf{k}$	is the intrinsic permeability of phase β (m^2)
$k_{r\beta}$	is the relative permeability of phase β.
P_β	is the pressure of phase β (Pa)
$\mathbf{g}$	is the gravitational acceleration (m s^{-2}) .

The integration is over an arbitrary sub-domain V_n of the flow system, which is bounded by the closed surface Γ_n. The left side is accumulation term denoting mass per unit volume, with κ labeling the mass components. q (kg m^{-3}) is the source term. The first tram of right side is mass flux term which was modified so that it has contributions from both the 'phase flux' and from diffusion.

In the case of two-phase flow, the unknown secondary parameters are the water saturation S_w, the gas saturation S_g, the relative permeability of water k_{rw}, and the relative permeability of gas k_{rg}. S_w is calculated from the gas saturation in the usual way.

$$S_w = 1 - S_g \tag{7}$$

In order to derive an expression for S_g, the Kozeny-Carman relationship, which quantifies the permeability in terms of some easily determined properties, was applied. The intrinsic permeability k of a sample is related to the average hydraulic radius r_h (m) of the flow pathways

$$k = \frac{\phi \tau r_h^2}{C} \tag{8}$$

where C is a dimensionless 'shape' factor. r_h is estimated from the capillary pressure P_c using the Young-Laplace equation

$$r_h = \frac{\sigma}{-P_c} \tag{9}$$

where σ is the surface tension (Pa m). Therefore, in the case of the gas phase in a bentonite sub-region (for which $\phi_g = S_g \phi$ and $k_g = k_{rg} k$), we assume that

$$S_g = \frac{C k_{rg} k \left(-P_c / \sigma \right)^2}{\phi \tau} \tag{10}$$

k_{rw} is able to be selected from any of the relative permeability functions programmed in TOUGH2.
The relative permeability of gas is zero until P_c exceeds a gas entry pressure at first time, P_e. The relative permeability of gas then increases, almost instantaneously, to

$$k_{rg}\left(t = t_e\right) = k_0 \tag{11}$$

where

t_e is the gas entry time (s);
k_0 is the value of the relative permeability of gas, k_{rg}, at gas entry.

After gas entry, the relative permeability of gas is taken to evolve with time. Then, as the excess gas pressure falls towards the resealing value, P_r, the relative permeability of gas tends to be zero

$$\frac{\partial k_{rg}}{\partial t} = -\lambda \left[k_{rg} - k_{\infty}(p_c) \right] \tag{12}$$

$$k_{\infty}(p_c) = k_0 \left(\frac{-P_c - P_r}{P_e - P_r} \right) \exp\left(4 \frac{-P_c - P_e}{G} \right) \tag{13}$$

where

λ	is a time-dependence constant (s^{-1});
P_e	is the excess gas pressure at which the gas enters (Pa);
P_r	is the excess gas pressure at the bentonite resealing (Pa);
G	is an elastic material constant (Pa).

A model of capillary dilation suggests that G is given by

$$G = \frac{E}{1+\nu} \tag{14}$$

where

E	is Young's Modulus (Pa);
ν	is Poisson's ratio.

There was no experimental data on the effect of stress condition on the porosity, so that it is assumed to be constant unless either the 'expansivity' or the 'compressibility' of the swelled bentonite has non-zero value.

(2) Simulation results

The above mentioned modified multi-phase flow simulator THUGH2 was applied for the simulation of the gas migration experiment on pure bentonite (Kunigel V1) sample. A procedure of the simulation of gas migration test by using the modified TOUGH2 is described below. Initially parameter values of initial condition of the upstream pressure P_g, and backpressure P_w, the intrinsic permeability **k**, the relative permeability of gas at gas entry k_0, the excess gas pressure at which the gas enters P_e and the excess gas pressure at the bentonite resealing were determined directly from the experimental results. Then an elastic material constant G is pre-set by literature data of Young's Modulus and Poisson's ratio. Following a number of manual adjustment to achieve behaviour of the gas out flow rate and the upstream pressure of the sample which resembled the experimental results, the values of a time-dependence constant λ, 'shape' factor C and an elastic material constant G were chosen.

As shown in Figure-10, the gas out flow behaviour of the gas migration test consisted of three regions which had different permeability by several orders of magnitude. In this simulation, the first two regions of gas out flow behaviour were calculated by changing the parameter values at the beginning of the second region, in other words, at the first peak value of permeability was observed. The latest region which might be caused by creating pathways at the interface between sample and test vessel was out of calculation here. The simulation is modelled using a line of 39 grid cells. The first cell has a length of 88.2 cm and represents the gas accumulator upstream of the sample. The bentonite sample itself is divided into 34 cells, the first 17 of length 1.0 mm and the next 17 of length reducing from 0.5 mm to 0.01

mm such that the discretisation is graded to give greater refinement at the downstream end). All the cells have a cross-section of 38 mmϕ. This calculation was carried out using the enhanced EOS3B module of TOUGH2.

The simulation results of first and the second region of the gas migration test are shown in Figure-15 and Figure-16 respectively. The chosen values of the parameters for the modified TOUGH2 are given in Table-4. In Figure-15, the level of agreement for the gas breakthrough time, history of the gas out flow rate which is relatively low and increasing moderately and even history of the upstream pressure is encouraging. In Figure-16, modified TOUGH2 calculation gives a good agreement with the first peak value of gas out flow rate, but the predicted behaviour of gas out flow reduction is significantly rapid compared with observed values. As all parameters were not adjusted in this fitting exercise, the parameter values listed in Table-4 should be regarded as tentative. A best fit procedure may improve the result of simulation. In ether way, the difficulty in representing extremely large and instantaneous increase of gas out flow may be one of the particular features of and also exist as restrictions on performance of REV (Representative Elementary Volume) model which requires discretised space and time for calculation.

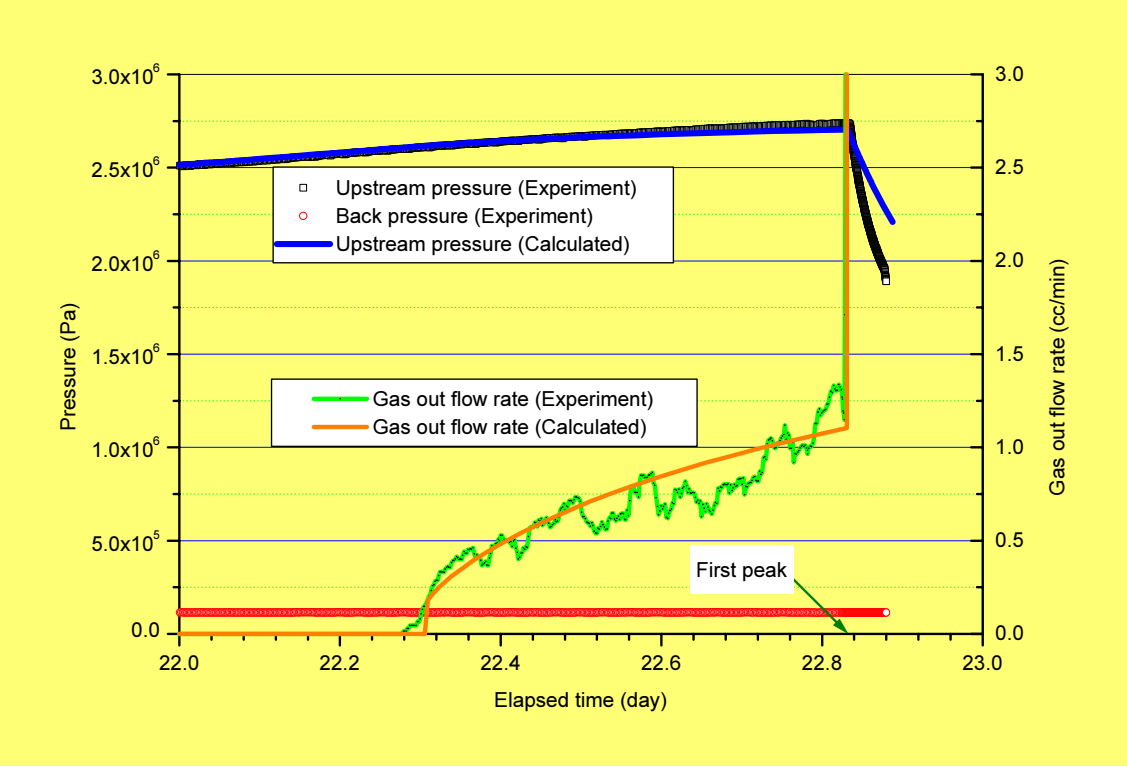

Figure-15 Results from a simulation of the gas injection test with the modified TOUGH2 (first phase of gas breakthrough)

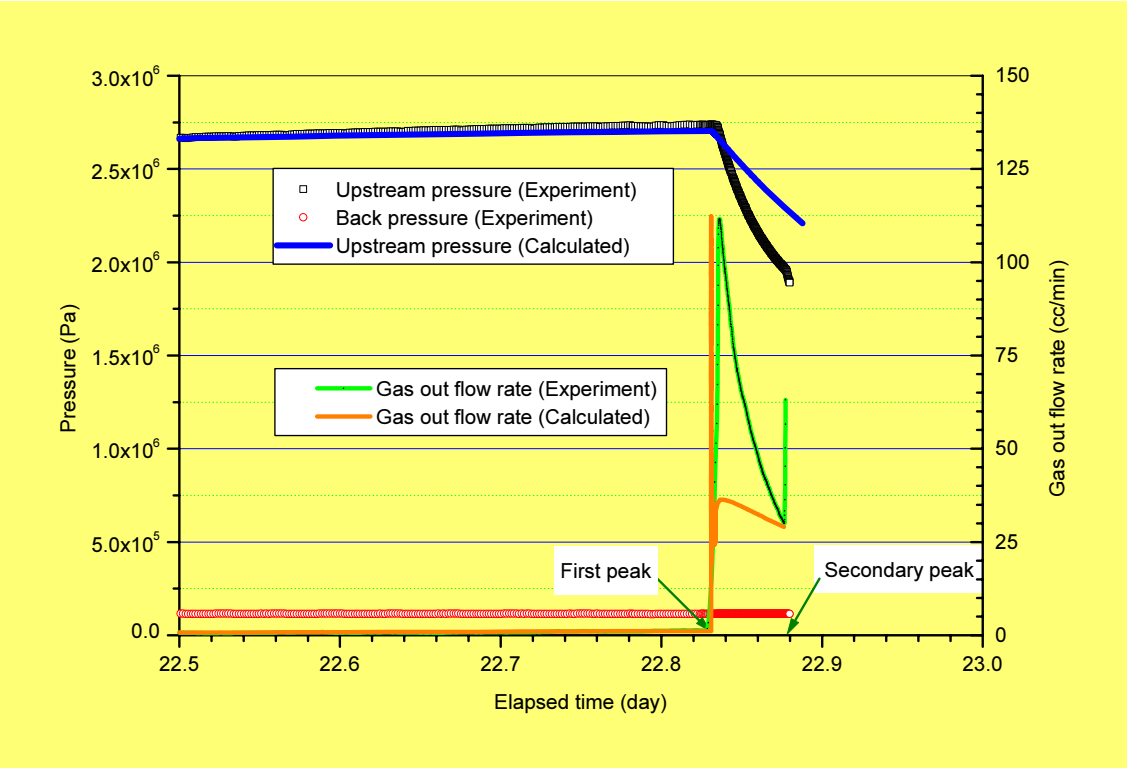

Figure-16 Results from a simulation of the gas injection test with the modified TOUGH2 (after the first peak of gas out flow)

Table-4 Parameter values

Parameter	Fixed value	Remark
Initial condition		
P_g	7.54 E+5 Pa	Experimental result
P_w	1.12 E+5 Pa	Experimental result
Pre-Breakthrough : First region		
k	5.0 E-20 m^2	Experimental result
k_0	1.0 E+1	Based on experimental result
P_e	2.48E+6 Pa	Experimental result
P_r	8.01E+5 Pa	Experimental result
G	3.1 E+6 Pa	Fitting parameter
λ	3.0 E-5	Fitting parameter
C	5.0 E-4	Fitting parameter
At First Peak : Second region		
k	5.0 E-20 m^2	Experimental result
k_0	3.75 E+5	Based on experimental result
P_e	2.48E+6 Pa	Experimental result
P_r	8.01E+5 Pa	Experimental result
G	3.1 E+6 Pa	Fitting parameter
λ	5.0 E-2	Fitting parameter
C	5.0 E-4	Fitting parameter

4. Conclusions

The knowledge obtained from previous studies are as follows, i) The gas permeabilities are 10^{-17} m^2 for the 30wt% sand mixtures at a dry density of 1.6 Mg m^{-3} and 10^{-20} to 10^{-21} m^2 for the bentonite (100%) at a dry density of 1.8 Mg m^{-3}, ii) The breakthrough pressure seems to be almost the same as the swelling pressure at constant volume condition, iii) Gas pathways created during the first gas injection period are closed due to bentonite swelling during the resaturation period.

For the recent experiment, two peaks of gas flow rate are obtained. In particular, maximum flow rate at secondary peak was approximately 1667 cc min^{-1}. This peak is probably indicative of generation of cracks in the specimen by particle displacement. Breakthrough pressure (2.5 MPa) is lager than the swelling pressure of the bentonite (swelling pressure is approximately 1.0 MP at a dry density of 1.6 Mg m^{-3}). It may be that there is a time lag between the gas pressure change in the clay and expansion of cracks due to large pumping rate (0.05 cc min^{-1}). The gas migration pathways are unstable due to stress condition in bentonite specimen and/or heterogeneity of specimen.

The distribution of bulk density in the specimen was measured to demonstrate that X-ray CT was reliable new technique for the non-destructive measurement of gas migration through bentonite specimen. The degree of X-ray attenuation depends on the bulk density of the bentonite specimen. The change in bulk density in this test specimen is not clear from this test case. But, these experimental results are probably indicative of migration along preferential pathway rather than uniform flow in the matrix of bentonite specimen.

A modified TOUGH2 simulator which has a gas flow model based on Kozeny-Carman relationship was developed and applied to simulate gas migration test in compacted bentonite. Although the results of the simulation reasonably agreed with obtained experimental data around gas breakthrough phenomenon, it has some difficulties to simulate “burst flow” which has extremely large and instantaneous increase of gas out flow. From these results, despite these difficulties, the continuous approach which can be conveniently coupled with phenomena of mechanical nature is one of the potential methods of describing gas migration in clay material.

References

Harrington, J F. and Horsemen, S T. : "Gas Migration in KBS-3 Buffer Bentonite, Sensitivity of test parameters to experimental boundary conditions", SKB TR 03-02, (2003).

JNC : "Second Progress Report on Research and Development for the Geological Disposal of HLW in Japan – Project to Establish the Scientific and Technical Basis for HLW Disposal in Japan –, Supporting Report 2, Repository Design and Engineering Technology", (2000).

Tanai, K., Kanno, T. and Gallé, C. : "Experimental Study of Gas permiabilities and Breakthrough pressures in Clays, Proceeding of the Scientific Basis of Nuclear Waste Management Conference Number XX, held in Boston", USA, December, 1996, Material Research Society, (1997).

Tanai, K., Yui. M., Umeki, H. and Yamamoto, M. : "The Treatment of Gas in the H12 Performance Assessment for HLW Disposal in Japan, Gas Generation and Migration in Radioactive Waste Disposal", Safety-relevant Issues, Workshop Proceedings, OECD/NEA, (2000).

Yamamoto, M. and Oba, T. : "Survey on the State of the Arts of Development of Gas Migration Models in Barrier System, document prepared by other institute", based on the trust contract, JNC TJ8440 2003-004 (2003) (in Japanese).

Pruess, K. : "TOUGH User's Guide", Nuclear Regulatory Commission Report NUREG/CR-4645 (also Lawrence Berkeley Laboratory Report 20700), (1987).

Pruess, K. : "TOUGH2 - A General-Purpose Numerical Simulator for Multiphase Fluid and Heat Flow", Lawrence Berkeley Laboratory Report 29400, (1991).

Dullien, F. A. L. : "Porous Media Fluid Transport and Pore Structure", Academic Press, (1979).

Fjaer, E., Holt, R. M., Horsrud, P., Raaen, A. M., Risnes, R. : "Petroleum Related Rock Mechanics", Elsevier, (1992).